

Nanomaterials and CO₂

Subjects: [Green & Sustainable Science & Technology](#)

Contributor: Francisco Jose Alguacil

Since CO₂ is an important component of gas emissions, its removal from gas streams is of the utmost importance to fulfill various environmental requirements. The technologies used to accomplish this removal are based mainly on absorption, as well as adsorption and membrane processing. Among the materials used in the above separation processes, materials in nano forms offer a potential alternative to other commonly used macromaterials.

CO₂

absorption

adsorption

membranes

1. Introduction

One of the main global concerns is related to the increasing concentration of CO₂ in the atmosphere, a consequence of the use of fossil fuels, boosting the greenhouse impact. There is no doubt that greenhouse gas emissions produce climate problems, resulting in challenges in reaching sustainable development. Greenhouse gas emissions are mainly a result of energy production (nearly 70% of global emissions). Many countries have considered the importance of reducing CO₂ emissions to fulfill environmental policies related to zero-carbon discharge, helping to reduce the presence of carbon in a number of sectors, with special interest in the energy sector. However, the time to achieve the transition from today's polluting energy production to a future of zero-emissions technology still seems long, and this is because there is a constant flux of information and developments to improve the capture of contaminant gases (CO₂, H₂S, CH₄, etc.) from gas streams in order to clean them and contribute to a better environment.

Among the technologies employed for this capture, and in the case of CO₂ specifically, absorption, adsorption, and membrane technologies are the most widely proposed. Several recent reviews on the utilization of these technologies have been published, including the use of membranes [\[1\]](#); MXene-based membranes [\[2\]](#); composite membranes [\[3\]\[4\]](#); microporous membranes composed of nanopores [\[5\]](#); nanomaterials [\[6\]\[7\]\[8\]\[9\]\[10\]\[11\]](#), and more specifically, graphene and its 2D nanomaterial derivatives [\[12\]](#); nanomaterials derived with support from artificial intelligence (AI) [\[13\]](#); kaolinite-based nanomaterials [\[14\]](#); MXene nanoderivatives [\[15\]](#); azobenzene-based supramolecular materials [\[16\]](#); carbon-bearing nanomaterials [\[17\]](#); nanobiotechnology using microalgae [\[18\]](#); nanomaterials for catalyst-assisted solvent regeneration in absorption processes using amine [\[19\]](#); and finally, some general reviews on technologies for CO₂ removal from gas streams [\[20\]\[21\]\[22\]\[23\]](#).

2. Nanomaterials and CO₂ Absorption

With quick kinetics, absorption techniques produce remarkable CO₂ removal (90%) from gases. The most-used absorbents to achieve this removal include amines, ammonia–water solutions, and alkali compounds. Both pre- and post-combustion processes can integrate these technologies into their general procedure. Besides physical absorption, chemical-driven absorption processes have three components: absorber, solvent, and stripper. Different pieces of equipment were used to capture CO₂, i.e., spray columns, packed beds, rotating packed beds, bubble columns, and tray tower absorber layouts.

The absorption of CO₂ on Al₂O₃/MeOH [24] was investigated, and the addition of a porous nickel metal foam increased CO₂ capture compared to pure MeOH; this increase was attributable to the forced bubble-breaking mechanism and the hydrodynamics in relation to the process. Moreover, there was a direct relation with the CO₂ absorption and the pressure and temperature used in the CO₂ capture process (**Figure 1**). For a constant pressure, increasing the temperature decreased the gas capture, whereas for a constant temperature, increasing the pressure produced a greater removal of CO₂ from the gas stream. Also, an increase (0.01–0.1 wt%) in the Al₂O₃ content is accompanied by an increase in the capture of CO₂ with the alcohol.

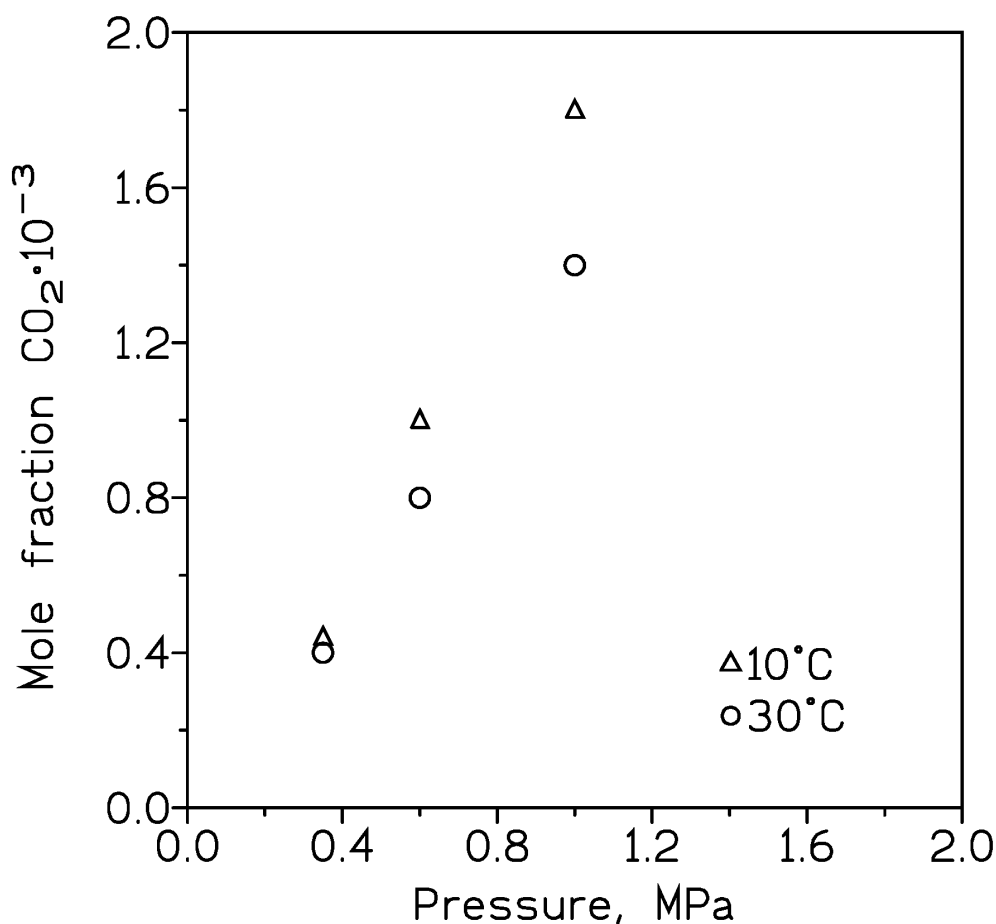


Figure 1. Approximate CO₂ removal in MeOH at various temperatures and pressures.

CO₂ capture by means of the addition of tetra-*n*-butyl ammonium bromide (TBAB) semiclathrate to graphite, forming a TBAB+graphite nanofluid, was investigated [25]. The TBAB+graphite nanofluid system increased CO₂

removal with respect to the use of the TBAB or TBAB+sodium dodecyl sulfate (SDS) solutions, with 0.2 wt% graphite nanoparticles being the best concentration for hydrate growth in the TBAB+graphite nanofluid.

A metal oxide solid acid catalyst for the catalytic regeneration of a CO₂-rich 5 M monoethanolamine (MEA) solution at 90 °C was used [26]. After the adsorption process and the formation of MEACOO⁻, carbamate decomposition occurred:



This was followed by protonated amine deprotonation and the formation of MEA, H₃O⁺, and H₂CO₃. The utilization of SO₄²⁻/ZrTiO_x allowed for a 99% increase in the CO₂ desorption rate and a 43% enhancement after continuous cycles.

The performance of single-walled, carbon-deficient silicon carbide nanotubes (Si₁₂C_{2-x}; X = 1; 2) in CO₂ capture was investigated [27]. The investigation concluded that Si₁₂C₁₁:Vc1 and Si₁₂C₁₀:Vc2 performed well for CO₂ removal and storage, surpassing the CO₂ capture efficiency of pristine SWSiCNT. The absorbent properties were due to the C vacancy effect of photoabsorption.

5,6-Dimethylbenzimidazole replaced 2-methylimidazole on the surface of ZIF-8 crystals via the shell–ligand exchange reaction (SLER) [28], improving the thermal stability of ZIF-8. At 40 °C, CO₂ uptake using ZIF-8-SLER-PLs increased 30% with respect to that of ZIF-8-PLs. CO₂ was loaded onto the modified absorbent via a physical absorption process.

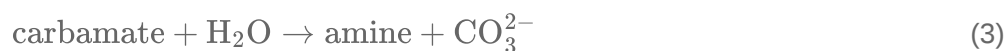
It was demonstrated [29] that the use of nano-SiO₂, with varying particle size, in glycerol solution had little effect on CO₂ removal; this capture increased with the increase in solid mass in the 0.05–0.15 wt% range, which was attributed to a better gas–liquid mass transfer area. The use of SiO₂ increased CO₂ desorption as consequence of the presence of more nucleation sites and the heating rate of the base fluid, generating bubbles.

MFCs (MgFe₂O₄@ZIF-62) containing various magnetic nanoparticle dosages (1–6 wt% of magnetic nanoparticles to ZIF-62 mass) were used in conjunction with a compatible non-penetrating solvent to form a magnetic porous liquid [30]. The use of this absorbent material allowed continuous CO₂ capture and release for up to three cycles.

Due to certain operational and economic considerations, there is a relatively urgent necessity to find alternatives to the use of amines for CO₂ capture [31]; amino acid salts can be one green alternative to the use of these amines. Thus, potassium L-cysteine for CO₂ capture from natural gas was investigated. Its physicochemical properties were measured at different temperatures (25–60 °C) and salt concentrations (5–30 wt%). Experimental results, at 40 °C and 20 bar, showed an important increment of CO₂ loading, from 7 to 15 mmol CO₂/g amino acid, with the increase of 10–30 wt% in the solvent concentration. CO₂ loading was attributable to the following reaction:



while carbonate formation occurred via the following reaction:



By the use of 9.01 wt% tetra butyl ammonium bromide (TBAB) mixed with water-soluble hydroxylated multiwalled carbon nanotube (MWCNTol) material, the formation of CO₂ hydrate was investigated [32]. It was concluded that MWCNTols had negligible influence on the CO₂ hydrate generation. The use of nanoparticles such as graphene nanoribbons and MWCNTols reduced the induction time, whereas addition of various nanoparticle dosages to the TBAB solution increased the final gas consumption, with a maximum increase of 10.44% in the 9.01 wt% TBAB + 0.08 wt% GN system.

Absorption and conversion of CO₂ by an amino-acid-based nanotechnology was described [33]. CO₂ was captured as bicarbonate nanomaterials, whereas the amino acid structure governed the formation of bicarbonate nanomaterials. Amino acids presented higher CO₂ absorption capacity and faster kinetics compared to the use of 30 wt% monoethanolamine.

Gold nanoparticles were decorated with 1,5,7-triazabicyclo [4.4.0] dec-5-ene and dispersed into methanol in order to capture CO₂ [34]. The photocatalyst consisted of two parts: (i) an organic shell responsible for CO₂ capture, and (ii) a plasmon-active metal nanoparticle core for activation of captured CO₂ and its involvement in the cycloaddition reaction. Results showed the efficiency of the procedure even at the temperature of -40 °C.

The mixture formed by NaP zeolite nanocrystals and 1-dodecyl-3-methylimidazolium chloride ([C₁₂mim][Cl]) ionic liquid was used for CO₂ removal in an isothermal high-pressure cell equipped with magnetic stirring [35]. Under various experimental conditions, it was found that 0.02 wt% of zeolite nanoparticles, 0.4 wt% of [C₁₂mim][Cl] ionic liquid, and 0.05 wt% of sodium dodecyl benzene sulfonate in nanofluids resulted in the highest CO₂ removal compared to other conditions. This CO₂ removal increased by increasing ionic liquid and surfactant concentration up to a limiting value near the critical micelle concentration.

Methyl-diethanolamine-based Fe₃O₄ improved CO₂ absorption compared to methyl-diethanolamine-based CuO, ZnO, and SiO₂, whereas CuO nanoparticles presented higher efficiency for CO₂ removal from gas-loaded absorbent [36].

Using 2-methylimidazole zinc salt (ZIF-8) modified by tetraethylenepentamine (TEPA), which provided pores, and 1-ethyl-3-methylimidazolium bis(trifluoro-methanesulfonyl)-imide ([EMIm][NTf₂]) ionic liquid, used as a sterically hindered diluent, an amine-functionalized type III porous liquid was formed [37]. It was found that with

30TEPA@ZIF-8 nanoparticles, the best CO₂ absorption capacity was obtained. Moreover, the CO₂ absorption loading of 0.124 mmol/g presented by 5-30TEPA@ZIF-8/[EMIm][NTf₂] was 4.43 times higher than the value obtained by the use of 5-0TEPA@ZIF-8/[EMIm][NTf₂], whereas a 745% increase of the absorption rate was reached.

A mixture of 26 mol% CO₂ and 74 mol% CH₄ was used to investigate the separation of both gases [38]. Silica nanoparticles, in KOH medium, modifying the surface of (3-aminopropyl) triethoxysilane (APTES) were utilized as additives. The best results were derived with silica and KOH-bearing nanofluids; with these components, improvements of 36% (gas consumption), 29% (separation factor), and 38% (recovery factor) resulted with respect to the use of pure water.

CO₂ geological sequestration by the use of silica aerogel nanofluid was investigated [39]. Using this material, non-dissolved CO₂ molecules were captured in the nanopores of the silica aerogel nanoparticles, increasing the solubility of CO₂ in the aqueous phase. Aerogel nanoparticles adsorbed at the CO₂-brine interface reduced the interfacial tension.

3. Nanomaterials and CO₂ Adsorption

Adsorption processing involves the use of a solid material on which CO₂ (and other gases and solutes) is captured by means of physical or chemical processes or a combination of both. Key parameters to yield the best adsorptive properties of the materials are: porosity, pore size, operational stability, presence of reactive groups towards CO₂ adsorption, etc., whereas the equipment used is usually described as a packed or fluidized bed.

The fabrication of carbon nanofibers (CNFs) via biaxial electrospinning was investigated [40]. Polymethylmethacrylate (PMMA) and polyacrylonitrile (PAN) were used as core and shell precursors, respectively. Further, Co₃O₄ nanoparticles were included in the PAN shell, increasing its roughness and surface area. The uniform distribution of Co₃O₄ resulted in a better flexibility of the hollow carbon nanofiber material (HCNF-Co), providing more vacant oxygen sites to increase CO₂ adsorption loading. HCNF-Co nanofibers exhibited CO₂ capture uptake of 3.28 mmol/g at 25 °C. Experimental results indicated that HCNF-Co had remarkable CO₂ selectivity (S = 26) over N₂.

Heterojunctions of Co₃O₄ with different morphologies and modified carbon nitride (CN) were investigated in order to optimize their properties to degrade CO₂ under UV-visible irradiation [41]. A solvothermal synthesis was used to fabricate the cobalt oxide from metal-organic framework structures, yielding ultrathin 2D Co₃O₄ nanosheets (Co₃O₄-NS). These nanosheets presented improved photocatalytic properties compared to those of the bulk Co₃O₄/CN composites. CO₂ reduction was improved due to (i) the match of the planar surface of CN and the 2D structure of Co₃O₄-NS, which resulted in a larger interface, and (ii) improvement in charge carrier lifetime.

The authors of [42] described the utilization of 2D nanomaterial MXenes and activated carbon (AC) to form sandwich-type materials and nanocomposites for CO₂ adsorption using a fixed-bed column. These investigations

included CO₂ breakthrough measurements at a fixed 15% CO₂ concentration, with an inlet flow rate at 200 mL/min and temperatures in the 25–55 °C range. The highest CO₂ adsorption load (near 9 mg/g) was yielded with AC/MXene sandwich adsorbent at 25 °C, which was nearly a 37% improvement in CO₂ adsorption capacity over the use of pristine AC. AC/MXene sandwich-type nanomaterials can be used, with a small loss of their CO₂ adsorption uptake, under various cyclic experiments.

ZIF-8 hollow nanospheres, for selective CO₂ separation and storage, were developed [43]. The optimum hollow ZIF-8 nanosphere material, with a uniform size distribution (**Figure 2**), had a CO₂ adsorption uptake of 2.24 mmol/g at 0 °C and 1.75 bar, selective (12.15) CO₂/N₂ separation, 1.5–1.75 wt% CO₂ storage capacity, and a reasonable stability, up to four CO₂ adsorption/desorption cycles, at 25 °C.

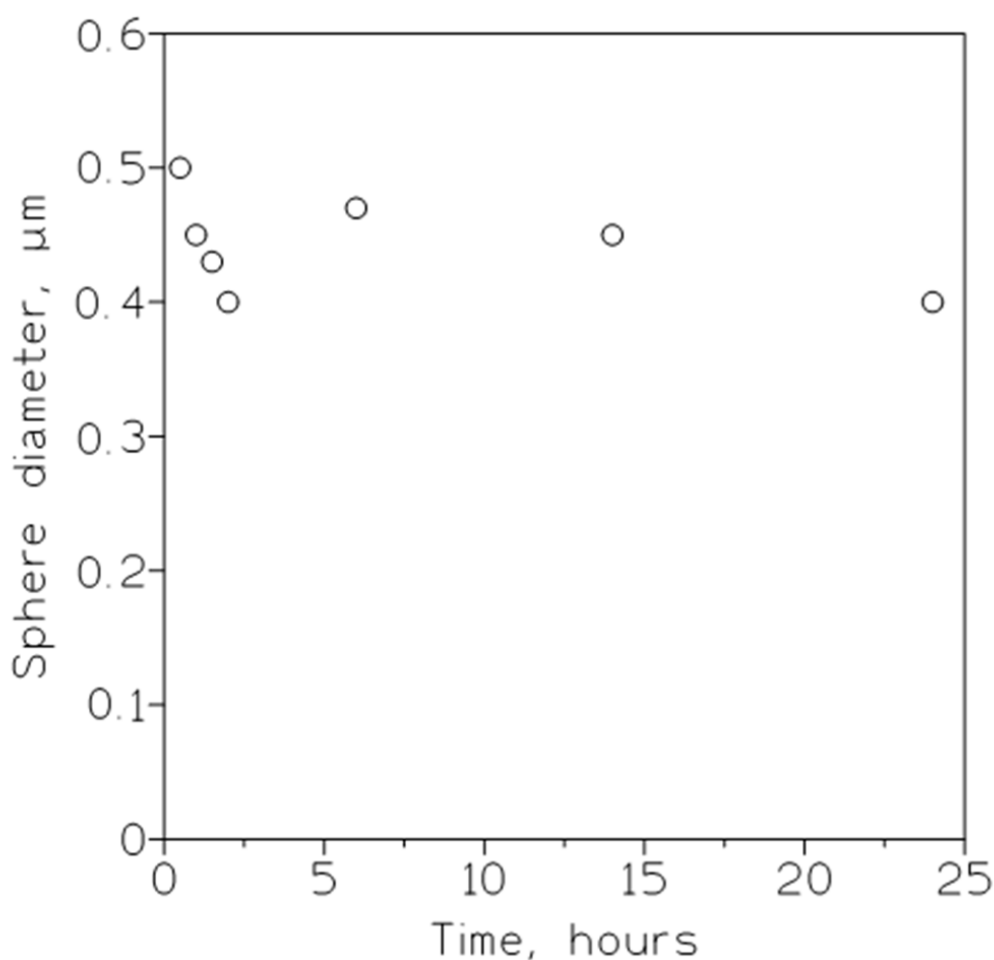


Figure 2. Influence of synthesis time on the average diameter of soft template hollow ZIF-8 nanospheres.

Surfactant/oil ratio: 75 g/L.

A heterogeneous catalyst comprising silver nanoparticles and a porous N-heterocyclic carbene polymer (Ag@POP-NL-3) was developed [44]. This nanomaterial has a regular distribution of silver nanoparticles and nitrogen activation groups. The catalyst presented good properties for the selective adsorption and activation of CO₂, allowing the conversion, under mild conditions, of low CO₂ (30 vol%) concentrations, as presented in lime kiln

waste gas, into cyclic carbonate. CO₂ was loaded onto the adsorbent by carboxylative cyclization of the gas with propargylic alcohols also present in the system.

The adsorption uptake of CO₂ on NaY@polyacrylate matrix was increased by 17.9% while H₂O adsorption uptake decreased by 36.6% compared to pristine NaY [45]. In addition, H₂O adsorption was reduced by 54.8% after adding ZIF into composites.

The authors of [46] described a maximum CO₂ loading (0.75 mmol/g) on triethylamine-doped rice husk silica nanoparticles, with an average increase in CO₂ adsorption with the increase (1 to 5 wt%) in the amine loading on the surface modifiers. Amine loadings greater than 5 wt% produced agglomeration of the particles which is detrimental with respect to CO₂ capture. CO₂ uptake corresponded to the Langmuir isotherm model.

The use of Zn-N pillar MOFs resulted in: CO₂ capture of 3.82 mmol/g (25 °C and 101 kPa), a selectivity CO₂/N₂ factor of 132, and stable structure (no change after exposure to 1000% RH environment for seven days) [47].

The performance of graphene oxide (GO)-coated zinc tetraphenylporphyrin (ZnTPP/GO) nanocomposites in the photocatalytic degradation of CO₂ was investigated [48]. The encapsulation of GO in ZnTPP nanocrystals promotes CO₂ adsorption, interfacial reaction, and stability and accelerates the separation of photoinduced carriers on ZnTPP (0.1 ps vs. 425.9 ps), the transportation from ZnTPP to GO (2.3 ps vs. 83.6 ps), and their final enrichment on GO.

A porous ZIF-11@ZIF-8 core-shell composite structure metal-organic framework was fabricated using the solvent-assisted linker exchange (SALE) procedure [49]. Adsorptions at 25 °C and equilibrium pressures up to 4 bar showed an increase (near 100%) in CO₂ adsorption uptake of ZIF-11@ZIF-8 nanoparticles (8.21 mmol/g) compared to the pristine ZIF-11 (4.35 mmol/g). Experimental results on gas uptake fitted well with the Langmuir isotherm equation. CO₂/N₂ and CO₂/CH₄ selectivities also increased by 131% and 92%, respectively.

Activated carbon (AC) was synthesized from date fruit seeds and chemically activated with KOH to improve CO₂ loading [50]. From thermogravimetric analyses, 94% and 67% higher average CO₂ capture loads were measured for KOH-promoted ACs compared to the original adsorbents. The activated carbon improved its fluidization by the use of hydrophobic silica nanoparticles (NPs). The SiO₂-decorated (2.5 wt%) modified ACs had a 45% higher bed expansion ratio, which was associated with the absence of bubbles and a homogeneous fluidized regime.

Mesoporous CeO₂, ZrO₂, and Ce-Zr composite nanoparticles with a large surface area were fabricated using the hydrothermal template-assisted synthesis procedure, and CO₂ adsorption properties of these materials were investigated under equilibrium and dynamic operations [51]. Better CO₂ adsorption was yielded for Ce-Zr nanomaterial due to the presence of strong O²⁻ base sites and many surface oxygen species. After five adsorption/desorption cycles, the composites presented a reasonable stability with a slight decrease in CO₂ adsorption uptakes in dry flow and in the presence of water vapor.

Treatment via surface N₂ plasma of zinc porphyrin (ZnTCPP) ultrathin nanosheets induced nitrogen vacancies (NVs) and resulted in a material with photocatalytic CO₂ reduction activity and selectivity [52]. It was shown that the photocatalytic activity of NVs-ZnTCPP can be attributed to nitrogen-vacancy-induced spin polarization by reducing the reaction barriers and inhibiting the recombination of photoexcited carriers.

It was reported [53] that CO₂ uptake (11.8 mmol/g (78% total adsorption)) after four cycles on a MOF-derived nano-CaO (average size of 100 nm) was due to high stability produced in the final material by the change in the original fiber-bundle-like MOF structure to nanosheets, and further to regular CaO spheres. CO₂ uptake onto the adsorbent corresponded to the following equation:



Lewis base and dual hydrogen bond donor (HBD) units were integrated into an organosilicon precursor, and triazine and hydrazo site co-modified periodic mesoporous organosilicas (THPMOs) were prepared via a hydrothermal self-assembly method [54]. The THPMOs had BET surface areas in the 699–876 m²/g range and low-pressure CO₂ adsorption loadings at 0 °C. If combined with tetrabutylammonium iodide (TBAI) ionic liquid, the mixture promoted the model cycloaddition of CO₂ in an effective form, with the gas fixed to epoxides.

In [55], nano-TiO₂ was added to cement pastes to investigate its performance regarding the CO₂ uptake rate. Prismatic samples with dimensions of 16 × 4 × 4 cm of 0.5 water/binder cement paste with and without nano-TiO₂ particles were used. CO₂ uptakes showed that nano-TiO₂ addition improves the CO₂ uptake rate of cement pastes, changing the pore structure and allowing the removal of more CO₂ at lower gas concentrations. CO₂ loaded similarly to Equation (4), but Ca(OH)₂ reacted with the gas to form CaCO₃ and water.

MIL-101(Cr)-NH₂ has higher CO₂ adsorption capacity than MIL-101(Fe)-NH₂ [56], whereas the adsorption of methane and nitrogen by MIL-101(Cr)-NH₂ is lower than the adsorption of these gases by MIL-101(Fe)-NH₂, leading to a higher selectivity of CO₂ over the two gases for MIL-101(Cr)-NH₂. At elevated temperature and pressure, the chemisorption mechanism is predominant, which is attributable to the performance of amines, which adsorbed more CO₂ at these higher temperatures and pressure. Gas adsorption was explained by the use of a hybrid equation between Langmuir and Khan models:

$$q = q_s \frac{P}{(1 + P)^n} + Q \frac{P}{(1 + P)^n} \quad (5)$$

where q_s , Q , and n represent the parameters of the model, with P being the pressure of the vapor phase at the equilibrium.

References

1. Yuan, Z.; Tang, J.; Chen, D.; Li, Y.; Hong, Z.; He, X. Membranes for hydrogen rainbow toward industrial decarbonization: Status, challenges and perspectives from materials to processes. *Chem. Eng. J.* 2023, 470, 144328.
2. Ahmad, I.; Alayande, A.B.; Jee, H.; Wang, Z.; Park, Y.-J.; Im, K.S.; Nam, S.Y. Recent progress of MXene-based membranes for high-performance and efficient gas separation. *Diam. Relat. Mater.* 2023, 135, 109883.
3. Dai, Y.; Niu, Z.; Luo, W.; Wang, Y.; Mu, P.; Li, J. A review on the recent advances in composite membranes for CO₂ capture processes. *Sep. Purif. Technol.* 2023, 307, 122752.
4. Luo, W.; Li, F.; Li, H.; Zhang, Z.; Zhang, X.; Liang, Y.; Huang, G. From 0D to 3D nanomaterial-based composite membranes for CO₂ capture: Recent advances and perspectives. *J. Environ. Chem. Eng.* 2023, 11, 110657.
5. Dai, Y.; Niu, Z.; Wang, Y.; Zhong, S.; Mu, P.; Li, J. Recent advances and prospect of emerging microporous membranes for high-performance CO₂ capture. *Sep. Purif. Technol.* 2023, 318, 123992.
6. Alli, Y.A.; Oladoye, P.O.; Ejeromedoghene, O.; Bankole, O.M.; Alimi, O.A.; Omotola, E.O.; Olanrewaju, C.A.; Philippot, K.; Adeleye, A.S.; Ogunlaja, A.S. Nanomaterials as catalysts for CO₂ transformation into value-added products: A review. *Sci. Total Environ.* 2023, 868, 161547.
7. Baena-Moreno, F.M.; Leventaki, E.; Riddell, A.; Wojtasz-Mucha, J.; Bernin, D. Effluents and residues from industrial sites for carbon dioxide capture: A review. *Environ. Chem. Lett.* 2023, 21, 319–337.
8. Hanifa, M.; Agarwal, R.; Sharma, U.; Thapliyal, P.C.; Singh, L.P. A review on CO₂ capture and sequestration in the construction industry: Emerging approaches and commercialised technologies. *J. CO₂ Util.* 2023, 67, 102292.
9. Li, H. CO₂ capture by various nanoparticles: Recent development and prospective. *J. Clean. Prod.* 2023, 414, 137679.
10. Segneri, V.; Trinca, A.; Libardi, N.; Colelli, L.; Micciancio, M.; Vilardi, G. Nanoparticles used for CO₂ capture by adsorption: A review. *Chem. Eng. Trans.* 2023, 101, 133–138.
11. Youns, Y.T.; Manshad, A.K.; Ali, J.A. Sustainable aspects behind the application of nanotechnology in CO₂ sequestration. *Fuel* 2023, 349, 128680.
12. Azni Farhana Mazri, N.; Arifutzzaman, A.; Kheireddine Aroua, M.; Ekhlasur Rahman, M.; Ali Mazari, S. Graphene and its tailoring as emerging 2D nanomaterials in efficient CO₂ absorption: A

- state-of-the-art interpretative review. *Alex. Eng. J.* 2023, 77, 479–502.
13. Chen, H.; Zheng, Y.; Li, J.; Li, L.; Wang, X. AI for nanomaterials development in clean energy and carbon capture, utilization and storage (CCUS). *ACS Nano* 2023, 17, 9763–9792.
 14. Chen, M.; Yang, T.; Han, J.; Zhang, Y.; Zhao, L.; Zhao, J.; Li, R.; Huang, Y.; Gu, Z.; Wu, J. The application of mineral kaolinite for environment decontamination: A review. *Catalysts* 2023, 13, 123.
 15. Cui, Y.; Zhu, J.; Tong, H.; Zou, R. Advanced perspectives on MXene composite nanomaterials: Types synthetic methods, thermal energy utilization and 3D-printed techniques. *iScience* 2023, 26, 105824.
 16. Younis, M.; Ahmad, S.; Atiq, A.; Farooq, M.A.; Huang, M.; Abbas, M. Recent progress in azobenzene-based supramolecular materials and applications. *Chem. Rec.* 2023, 23, e202300126.
 17. Zhu, W.; Yue, Y.; Wang, H.; Zhang, B.; Hou, R.; Xiao, J.; Huang, X.; Ishag, A.; Sun, Y. Recent advances on energy and environmental application of graphitic carbon nitride (g-C₃N₄)-based photocatalysts: A review. *J. Environ. Chem. Eng.* 2023, 12, 110164.
 18. de Moraes, M.G.; Vargas, B.P.; da Silva Vaz, B.; Cardias, B.B.; Costa, J.A.V. Advances in the synthesis and applications of nanomaterials to increase CO₂ biofixation in microalgal cultivation. *Clean Technol. Environ. Policy* 2023, 25, 617–632.
 19. Waseem, M.; Al-Marzouqi, M.; Ghasem, N. A review of catalytically enhanced CO₂-rich amine solutions regeneration. *J. Environ. Chem. Eng.* 2023, 11, 110188.
 20. Chowdhury, S.; Kumar, Y.; Shrivastava, S.; Patel, S.K.; Sangwai, J.S. A review on the recent scientific and commercial progress on the direct air capture technology to manage atmospheric CO₂ concentrations and future perspectives. *Energy Fuels* 2023, 37, 10733–10757.
 21. Jaiswar, G.; Dabas, N.; Chaudhary, S.; Jain, V.P. Progress in absorption of environmental carbon dioxide using nanoparticles and membrane technology. *Int. J. Environ. Sci. Technol.* 2023, 20, 10385–10404.
 22. Peu, S.D.; Das, A.; Hossain, M.S.; Akanda, M.A.; Akanda, M.M.; Rahman, M.; Miah, M.N.; Das, B.K.; Islam, A.R.; Salah, M.M. A comprehensive review on recent advancements in absorption-based post combustion carbon capture technologies to obtain a sustainable energy sector with clean environment. *Sustainability* 2023, 15, 5827.
 23. Zhang, C.; Zhang, X.; Su, T.; Zhang, Y.; Wang, L.; Zhu, X. Modification schemes of efficient sorbents for trace CO₂ capture. *Renew. Sustain. Energy Rev.* 2023, 18, 113473.
 24. Boldoo, T.; Ham, J.; Cho, H. Evaluation of CO₂ absorption characteristics of low cost Al₂O₃/MeOH nanoabsorbent using porous nickel foam for high efficiency CO₂ absorption system.

- J. Clean. Prod. 2023, 384, 135624.
25. Ge, B.-B.; Yan, J.; Zhong, D.-L.; Lu, Y.-Y.; Li, X.-Y. CO₂ capture enhancement by forming tetra-n-butyl ammonium bromide semicrathrate in graphite nanofluids. *Can. J. Chem. Eng.* 2023, 101, 4128–4137.
 26. Geng, Z.; Yang, Y.; Wang, Y.; Zhu, T.; Xu, W. Catalytic regeneration of amine-based absorbents for CO₂ capture: The effect of acidic sites and accessibility. *Sep. Purif. Technol.* 2023, 327, 124889.
 27. Itas, Y.S.; Razali, R.; Tata, S.; Kolo, M.; Lawal, A.; Alrub, S.A.; El Ghouli, J.; Khandaker, M.U. DFT studies on the effects of C vacancy on the CO₂ capture mechanism of silicon carbide anotubes photocatalyst (Si₁₂C₁₂-X; X = 1; 2). *Silicon* 2023, 1–11.
 28. Jin, G.; Wang, H.; Zhang, K.; Zhang, H.; Fan, J.; Wang, J.; Guo, D.; Wang, Z. ZIF-8 based porous liquids with high hydrothermal stability for carbon capture. *Mater. Today Commun.* 2023, 36, 106820.
 29. Li, Y.; Lu, H.; Liu, Y.; Wu, K.; Zhu, Y.; Liang, B. CO₂ absorption and desorption enhancement by nano-SiO₂ in DBU-glycerol solution with high viscosity. *Sep. Purif. Technol.* 2023, 309, 122983.
 30. Mahdavi, H.; Sadiq, M.M.; Smith, S.J.D.; Mulet, X.; Hill, M.R. Underlying potential evaluation of the real-process applications of magnetic porous liquids. *J. Mater. Chem. A* 2023, 11, 16846–16853.
 31. Tengku Hassan, T.N.A.; Mohd Shariff, A.; Abd Aziz, N.F.; Mustafa, N.F.A.; Tan, L.S.; Abdul Halim, H.N.; Mohamed, M.; Hermansyah, H. Aqueous potassium salt of L-cysteine as potential CO₂ removal solvent: An investigation on physicochemical properties and CO₂ loading capacity. *Sustainability* 2023, 15, 11558.
 32. Wang, S.-L.; Xiao, Y.-Y.; Zhou, S.-D.; Jiang, K.; Yu, Y.-S.; Rao, Y.-C. Synergistic effect of water-soluble hydroxylated multi-wall carbon nanotubes and graphene nanoribbons coupled with tetra butyl ammonium bromide on kinetics of carbon dioxide hydrate formation. *Energies* 2023, 16, 5831.
 33. Wang, X.; Bao, Z.; Akhmedov, N.G.; Hopkinson, D.; Hoffman, J.; Duan, Y.; Egbebi, A.; Resnik, K.; Li, B. Unique biological amino acids turn CO₂ emission into novel nanomaterials with three switchable product pathways. *Environ. Technol. Innov.* 2023, 32, 103279.
 34. Zabelina, A.; Dedek, J.; Guselnikova, O.; Zabelin, D.; Trelin, A.; Miliutina, E.; Kolska, Z.; Siegel, J.; Svorcik, V.; Vana, J.; et al. Photoinduced CO₂ conversion under Arctic conditions—the high potential of plasmon chemistry under low temperature. *ACS Catal.* 2023, 13, 3830–3840.
 35. Zare, A.; Darvishi, P.; Lashanizadegan, A.; Zerafat, M. Theoretical and experimental investigation of CO₂ solubility in nanofluids containing NaP zeolite nanocrystals and ionic liquid. *Can. J. Chem. Eng.* 2023, 101, 3925–3936.

36. Zarei, F.; Keshavarz, P. Intensification of CO₂ absorption and desorption by metal/non-metal oxide nanoparticles in bubble columns. *Environ. Sci. Pollut. Res.* 2023, 30, 19278–19291.
37. Zhao, X.; Ding, Y.; Ma, L.; Zhu, X.; Wang, H.; Cheng, M.; Liao, Q. An amine-functionalized strategy to enhance the CO₂ absorption of type III porous liquids. *Energy* 2023, 279, 127975.
38. Khanmohammadian, E.; Mohammadi, M.; Hashemi, R.; Eslami, S.; Reza Ehsani, M. Improvement of gas hydrate-based CO₂ capture from CH₄/CO₂ mixture using silica and modified silica nanoparticles in the presence of potassium hydroxide. *Fuel* 2023, 334, 126458.
39. Lu, T.; Li, Z.; Du, L. Enhanced CO₂ geological sequestration using silica aerogel nanofluid: Experimental and molecular dynamics insights. *Chem. J.* 2023, 474, 145566.
40. Ali, N.; Babar, A.A.; Wang, X.; Yu, J.; Ding, B. Hollow, porous, and flexible Co₃O₄-doped carbon nanofibers for efficient CO₂ capture. *Adv. Eng. Mater.* 2023, 25, 2201335.
41. Anagnostopoulou, M.; Zindrou, A.; Cottineau, T.; Kafizas, A.; Marchal, C.; Deligiannakis, Y.; Keller, V.; Christoforidis, K.C. MOF-derived defective Co₃O₄ nanosheets in carbon nitride nanocomposites for CO₂ photoreduction and H₂ production. *ACS Appl. Mater. Interfaces* 2023, 15, 6817–6830.
42. Arifutzzaman, A.; Musa, I.N.; Aroua, M.K.; Saidur, R. MXene based activated carbon novel nano-sandwich for efficient CO₂ adsorption in fixed-bed column. *J. CO₂ Util.* 2023, 68, 102353.
43. Butt, F.S.; Lewis, A.; Rea, R.; Mazlan, N.A.; Chen, T.; Radacsi, N.; Mangano, E.; Fan, X.; Yang, Y.; Yang, S.; et al. Highly-controlled soft-templating synthesis of hollow ZIF-8 nanospheres for selective CO₂ separation and storage. *ACS Appl. Mater. Interfaces* 2023, 15, 31740–317545.
44. Chen, P.-B.; Yang, J.-W.; Rao, Z.-X.; Wang, Q.; Tang, H.-T.; Pan, Y.-M.; Liang, Y. Efficient in-situ conversion of low-concentration carbon dioxide in exhaust gas using silver nanoparticles in N-heterocyclic carbene polymer. *J. Colloid Interface Sci.* 2023, 652, 866–877.
45. Chi, S.; Ye, Y.; Zhao, X.; Liu, J.; Jin, J.; Du, L.; Mi, J. Porous molecular sieve polymer composite with high CO₂ adsorption efficiency and hydrophobicity. *Sep. Purif. Technol.* 2023, 307, 122738.
46. Giraldo, L.J.; Medina, O.E.; Ortiz-Perez, V.; Franco, C.A.; Cortes, F.B. Enhanced carbon storage process from flue gas streams using rice husk silica nanoparticles: An approach in shallow coal bed methane reservoirs. *Energy Fuels* 2023, 37, 2945–2959.
47. Gu, Y.-M.; Wang, Y.-H.; Zhao, S.-S.; Fan, H.-J.; Liu, X.-W.; Lai, Z.; Wang, S.-D. N-donating and water-resistant Zn-carboxylate frameworks for humid carbon dioxide capture from flue gas. *Fuel* 2023, 336, 126793.
48. He, Y.; Wang, Z.; Cao, A.; Xu, X.; Li, J.; Zhang, B.; Kang, L. Construction of graphene oxide-coated zinc tetraphenylporphyrin nanostructures for photocatalytic CO₂ reduction to highly selective CH₄ product. *J. Colloid Interface Sci.* 2023, 638, 123–134.

49. Hosseini, S.R.; Omidkhah, M.; Mehri Lihgyan, Z.; Norouzbahari, S.; Ghadimi, A. Synthesis, characterization, and gas adsorption performance of an efficient hierarchical ZIF-11@ZIF-8 core–shell metal–organic framework (MOF). *Sep. Purif. Technol.* 2023, 307, 122679.
50. Iranvandi, M.; Tahmasebpour, M.; Azimi, B.; Heidari, M.; Pevida, C. The novel SiO₂-decorated highly robust waste-derived activated carbon with homogeneous fluidity for the CO₂ capture process. *Sep. Purif. Technol.* 2023, 306, 122625.
51. Issa, G.; Kormunda, M.; Tumurbaatar, O.; Szegedi, A.; Kovacheva, D.; Karashanova, D.; Popova, M. Impact of Ce/Zr ratio in the nanostructured ceria and zirconia composites on the selective CO₂ adsorption. *Nanomaterials* 2023, 13, 2428.
52. Jin, Z.; Zhang, J.; Qiu, J.; Hu, Y.; Di, T.; Wang, T. Nitrogen vacancy-induced spin polarization of ultrathin zinc porphyrin nanosheets for efficient photocatalytic CO₂ reduction. *J. Colloid Interface Sci.* 2023, 652, 122–131.
53. Liu, Z.; Lu, Y.; Wang, C.; Zhang, Y.; Jin, X.; Wu, J.; Wang, Y.; Zeng, J.; Yan, Z.; Sun, H.; et al. MOF-derived nano CaO for highly efficient CO₂ fast adsorption. *Fuel* 2023, 340, 127476.
54. Liu, M.; Ma, C.; Cheng, X.; Gao, K.; Zhang, G.; Wang, D.; Liu, F. New insight into multiple hydrogen-bond networks of functional organosilicas system for collaborative transformation of CO₂ under mild conditions. *Sep. Purif. Technol.* 2023, 317, 123937.
55. Lopez-Arias, M.; Moro, C.; Francioso, V.; Elgaali, H.H.; Velay-Lizancos, M. Effect of nanomodification of cement pastes on the CO₂ uptake rate. *Constr. Build. Mater.* 2023, 404, 133165.
56. Mahdipour, H.R.; Ebrahimi, R.; Ganji Babakhani, E.; Halladj, R.; Safari, N.; Ganji, H. Investigating the selective adsorption of CO₂ by MIL-101(Cr)-NH₂ and modeling the equilibrium data using a new three-parameter isotherm. *Colloids Surf. A Physicochem. Eng. Asp.* 2023, 675, 131971.

Retrieved from <https://encyclopedia.pub/entry/history/show/121273>